

A New Approach to Probe Non-Standard Interactions in Atmospheric Neutrino Experiments

(JHEP 04 (2021) 159, arXiv: 2101.02607)

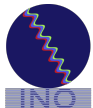
Anil Kumar

**Research Scholar, India-based Neutrino Observatory (INO)
(Institute of Physics, Bhubaneswar, India)**

Collaborators: Amina Khatun, Sanjib Kumar Agarwalla, Amol Dighe

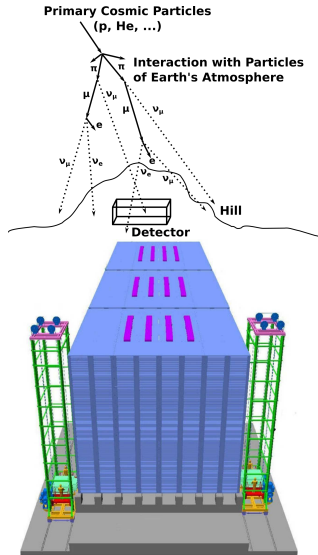


Sept 5, 2021
HEP-PHENO School (Online)
Aug 31 to Sept 12, 2021



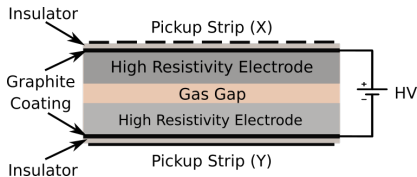
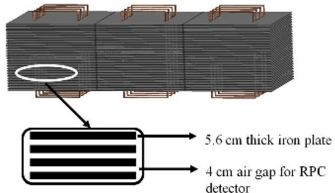
Iron Calorimeter Detector (ICAL) at INO¹

- **ICAL@INO:** 50 kton magnetized iron calorimeter detector at the proposed India-based Neutrino Observatory (INO)
- **Location:** Bodi West Hills, Theni District, Tamil Nadu, India
- **Aim:** To determine mass ordering and precision measurement of atmospheric oscillation parameters.
- **Source:** Atmospheric neutrinos and antineutrinos in the multi-GeV range of energies over a wide range of baselines.
- **Uniqueness:** Charge identification capability helps to distinguish μ^- and μ^+ and hence, ν_μ and $\bar{\nu}_\mu$
- **Muon energy range:** 1 – 25 GeV, **Muon energy resolution:** $\sim 10\%$
- **Baselines:** 15 – 12000 km, **Muon zenith angle resolution:** $\sim 1^\circ$



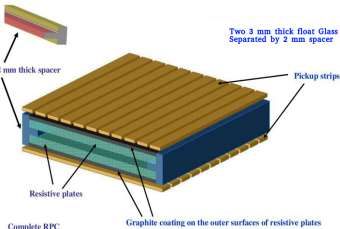
¹Pramana - J Phys (2017) 88 : 79, arXiv:1505.07380

ICAL Design and Specifications



| ICAL | |
|----------------------|----------------------|
| No. of modules | 3 |
| Module dimension | 16 m × 16 m × 14.5 m |
| Detector dimension | 48 m × 16 m × 14.5 m |
| No. of layers | 151 |
| Iron plate thickness | 5.6 cm |
| Gap for RPC trays | 4.0 cm |
| Magnetic field | 1.5 Tesla |

| RPC | |
|------------------------------------|-------------------|
| RPC unit dimension | 2 m × 2 m |
| Readout strip width | 3 cm |
| No. of RPC units/Layer/Module | 64 |
| Total no. of RPC units | ~ 30,000 |
| No. of electronic readout channels | 3.9×10^6 |

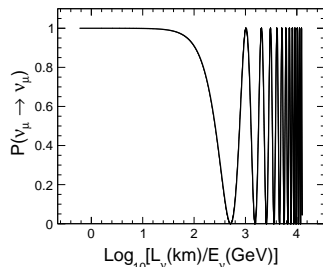


Resistive plate chamber (RPC) (active element) sandwiched between iron plates (passive element)

Oscillation Dip in Muon Neutrino Survival Probability

The L/E dependence of survival probability $P(\nu_\mu \rightarrow \nu_\mu)$ in two-flavor oscillation is given as:

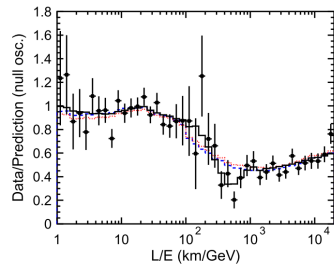
$$P(\nu_\mu \rightarrow \nu_\mu) = 1 - \sin^2 2\theta_{23} \cdot \sin^2 \left(1.27 \cdot |\Delta m_{32}^2| (\text{eV}^2) \cdot \frac{L_\nu (\text{km})}{E_\nu (\text{GeV})} \right)$$



For $\theta_{23} = 45^\circ$ and $\Delta m_{32}^2 = 2.4 \times 10^{-3}$ eV², $P(\nu_\mu \rightarrow \nu_\mu) = 0$ when

$$\frac{1.27 \Delta m_{32}^2 L_\nu}{E_\nu} = \frac{\pi}{2}$$

$$\frac{L_\nu}{E_\nu} = 515.35 \text{ km/GeV} \quad \& \quad \log_{10} \left(\frac{L_\nu}{E_\nu} \right) = 2.71$$



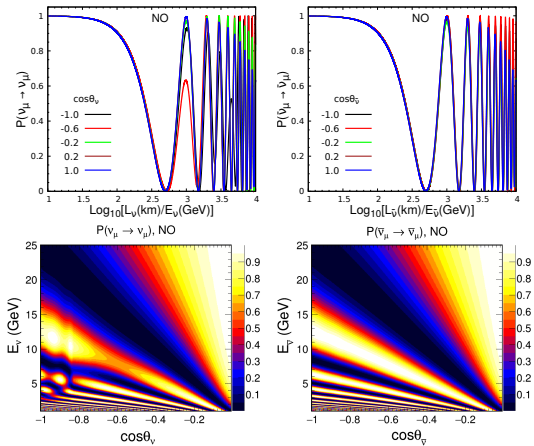
The Super-K experiment was the first experiment to confirm the sinusoidal L/E dependence of the ν_μ survival probability by observing a dip around $L/E = 500 \text{ km/GeV}$.

(Phys. Rev. Lett. 93 (2004) 101801)

Oscillation Dip and Oscillation Valley in Neutrino

Three-flavor oscillation framework in the presence of matter (PREM profile)

- **Oscillation dip** can be observed around $\log_{10}(L_\nu/E_\nu) = 2.7$
- Matter effect in $P(\nu_\mu \rightarrow \nu_\mu)$ for the case of neutrino (due to normal ordering) can be observed around $\log_{10}(L_\nu/E_\nu) = 3.0$
- The **oscillation valley** can be seen as dark blue diagonal band.



$L_\nu = \sqrt{(R+h)^2 - (R-d)^2 \sin^2 \theta_\nu} - (R-d) \cos \theta_\nu$, where R , h , and d are the radius of Earth (6371 km), the average height from the Earth surface at which neutrinos are created (15 km), and the depth of the detector underground (0 km), respectively.

Event generation at ICAL

In this analysis, we use:

- Neutrino Flux at INO site (Theni)
- Unoscillated neutrino events generation using NUANCE⁴ for ICAL geometry
- Three flavor matter oscillation with PREM⁵ profile
- Migration matrices⁶ for detector response to muons obtained from ICAL-GEANT4 simulation

The values of the benchmark oscillation parameters used in this analysis.

| $\sin^2 2\theta_{12}$ | $\sin^2 \theta_{23}$ | $\sin^2 2\theta_{13}$ | $ \Delta m_{32}^2 \text{ (eV}^2)$ | $\Delta m_{21}^2 \text{ (eV}^2)$ | δ_{CP} | Mass Ordering |
|-----------------------|----------------------|-----------------------|------------------------------------|----------------------------------|---------------|---------------|
| 0.855 | 0.5 | 0.0875 | 2.46×10^{-3} | 7.4×10^{-5} | 0 | Normal (NO) |

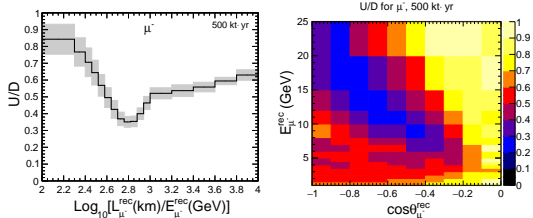
⁴D. Casper, Nucl. Phys. B Proc. Suppl. 112 (2002) 161

⁵A.M. Dziewonski et al. Phys.Earth Planet.Interiors 25 (1981) 297-356

⁶Animesh Chatterjee et al. 2014 JINST 9 P07001, arXiv:1405.7243

Oscillation dip and valley in ν_μ survival probability

- The first oscillation minima results in **oscillation dip** in L/E and **oscillation valley** in (L,E) plane.
- The U/D ratio of the reconstructed muon events is a good proxy for ν_μ survival probability.
- The U/D ratio automatically cancels most of the systematic uncertainties.



Anil Kumar et. al. EPJC 81 (2021) 2, 190, arXiv:2006.14529

U/D ratio (defined for $\cos \theta_\mu^{\text{rec}} < 0$)

$$U/D(E_\mu^{\text{rec}}, \cos \theta_\mu^{\text{rec}}) \equiv \frac{N(E_\mu^{\text{rec}}, -|\cos \theta_\mu^{\text{rec}}|)}{N(E_\mu^{\text{rec}}, +|\cos \theta_\mu^{\text{rec}}|)},$$

where $N(E_\mu^{\text{rec}}, \cos \theta_\mu^{\text{rec}})$ is the number of events with energy E_μ^{rec} and zenith angle θ_μ^{rec} .

Neutral current Non-Standard Interactions (NSI)

Neutral current NSI in propagation through matter.

$$\mathcal{L}_{\text{NC-NSI}} = -2\sqrt{2}G_F \varepsilon_{\alpha\beta}^{Cf} (\bar{v}_\alpha \gamma^\rho P_L v_\beta) (\bar{f} \gamma_\rho P_C f)$$

where, $P_L = (1 - \gamma_5)/2$, $P_R = (1 + \gamma_5)/2$, and $C = L, R$.

$$\varepsilon_{\alpha\beta} = \sum_{f=e,u,d} \frac{V_f}{V_{CC}} \left(\varepsilon_{\alpha\beta}^{Lf} + \varepsilon_{\alpha\beta}^{Rf} \right)$$

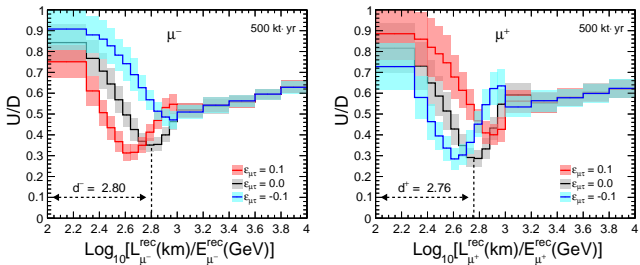
where, $V_{CC} = \sqrt{2}G_F N_e$, $V_f = \sqrt{2}G_F N_f$, $f = e, u, d$.

$$H_{mat} = \sqrt{2}G_F N_e \begin{pmatrix} 1 + \varepsilon_{ee} & \varepsilon_{e\mu} & \varepsilon_{e\tau} \\ \varepsilon_{e\mu}^* & \varepsilon_{\mu\mu} & \varepsilon_{\mu\tau} \\ \varepsilon_{e\tau}^* & \varepsilon_{\mu\tau}^* & \varepsilon_{\tau\tau} \end{pmatrix}$$

In atmospheric neutrinos, $\mu - \tau$ channel is dominant, hence, we choose to study about $\varepsilon_{\mu\tau}$ (only real values)

$$H_{mat} = \sqrt{2}G_F N_e \begin{pmatrix} 1 & 0 & 0 \\ 0 & 0 & \varepsilon_{\mu\tau} \\ 0 & \varepsilon_{\mu\tau}^* & 0 \end{pmatrix}$$

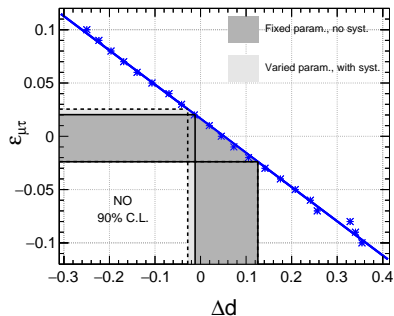
Shift in dip location in reconstructed muon observables



- Statistical uncertainty calculated using 100 simulated sets of 10-year data.
- The location of dip d^- or d^+ depends on magnitude as well as sign of $\varepsilon_{\mu\tau}$.
- d^- and d^+ shift in the opposite direction due to $\varepsilon_{\mu\tau}$.
- d^- and d^+ shift in the same direction due to change in Δm_{32}^2 .
- New variable $\Delta d = d^- - d^+$ depends on $\varepsilon_{\mu\tau}$ but independent of Δm_{32}^2 (true).

Constraints on $\varepsilon_{\mu\tau}$ from measurement of Δd

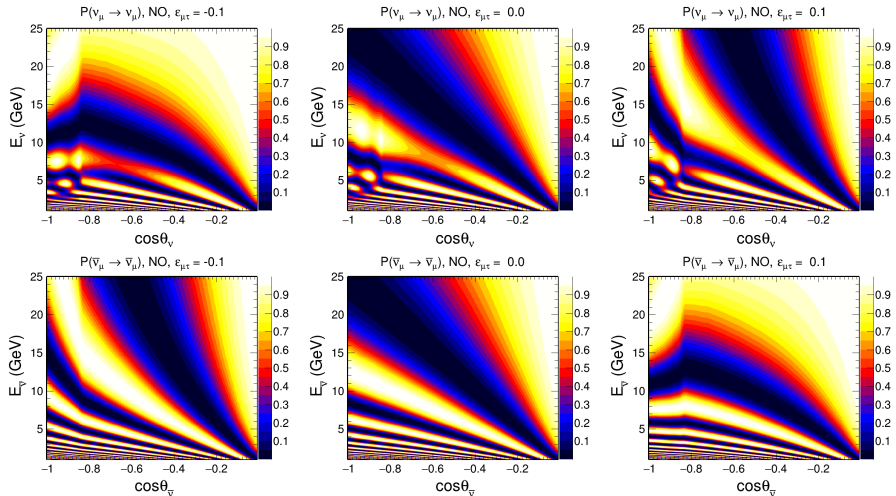
- We calibrate $\varepsilon_{\mu\tau}$ with respect to Δd using 1000 yr Monte Carlo.
- The 90% C.L. are obtained using multiple simulated sets of 10-year data.
- **Variation over oscillation parameters:** 20 random choices of oscillation parameters for each 10-year simulated data set, according to the Gaussian distribution using σ from current global fit.
- **Systematics errors with Gaussian distributions:** overall flux normalization (20%), cross sections (10%), energy dependence (5%), zenith angle dependence (5%), and overall systematics (5%).



90% C.L.:

- Fixed param., no syst: $-0.024 < \varepsilon_{\mu\tau} < 0.020$
- Varied param., with syst.: $-0.025 < \varepsilon_{\mu\tau} < 0.024$

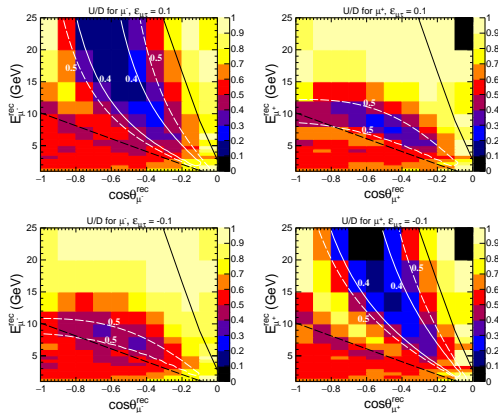
Oscillation valley in neutrino survival probability



The presence of NSI results in the curvature of oscillation valley (dark blue diagonal band).

Curvature of Oscillation Valley in Reconstructed Muon Observables

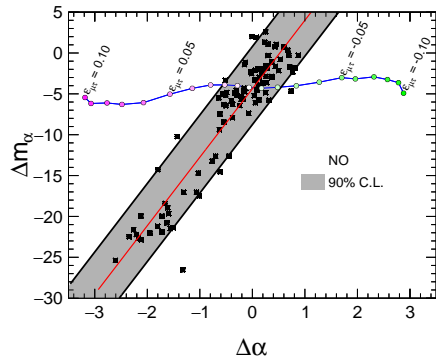
- Mean of 100 U/D distribution for 10 year data in presence of NSI ($\varepsilon_{\mu\tau} = -0.1$ and 0.1).
- Solid black and dashed black lines show conical cut of $\log_{10} L/E = 2.2$ and $\log_{10} L/E = 3.1$ respectively which includes bins used for fitting.
- For $\Delta_{21}^2 L/4E \rightarrow 0$, $\theta_{13} = 0$, and $\theta_{23} = 45^\circ$ ([arXiv:1410.6193](#)),
 $P(\nu_\mu \rightarrow \nu_\mu) = \cos^2 \left[L \left(\frac{\Delta m_{32}^2}{4E} + \varepsilon_{\mu\tau} V_{CC} \right) \right]$
- Solid white and dashed white lines show contours with U/D ratio of 0.4 and 0.5 respectively for fitted function $f(x, y) = z_0 + N_0 \cos^2 \left(m_\alpha \frac{x}{y} + \alpha x^2 \right)$.



The parameter α is the measure of the curvature of oscillation valley and contains the information about $\varepsilon_{\mu\tau}$.

Constraints on $\varepsilon_{\mu\tau}$ using curvature of oscillation valley

$$\Delta m_\alpha = m_{\alpha^-} - m_{\alpha^+} \text{ and } \Delta\alpha = \alpha^- - \alpha^+$$



90% C.L.:

- Fixed param., no syst: $-0.022 < \varepsilon_{\mu\tau} < 0.021$
- Varied param., with syst.: $-0.024 < \varepsilon_{\mu\tau} < 0.020$

Conclusion

- ICAL has good reconstruction efficiency for μ^- and μ^+ over a wide range of energy and direction.
- Oscillation dip and oscillation valley can be observed in reconstructed muon observables at ICAL.
- We propose a new approach to utilize oscillation dip and oscillation valley to probe neutral-current NSI parameter $\varepsilon_{\mu\tau}$.
- A new variable representing shift in location of dip for μ^- and μ^+ is used to constrain NSI parameter $\varepsilon_{\mu\tau}$.
- The contrast in curvature of valley for μ^- and μ^+ is used to constrain NSI parameter $\varepsilon_{\mu\tau}$.

Acknowledgement: We acknowledge financial support from the Department of Atomic Energy (DAE), Department of Science and Technology (DST), Govt. of India, and the Indian National Science Academy (INSA).

Thank you

Backup: Neutrino Oscillations in Three-flavor Framework

$$\nu_\alpha = \sum_i U_{\alpha i} \nu_i$$

$$U = \begin{pmatrix} 1 & 0 & 0 \\ 0 & c_{23} & s_{23} \\ 0 & -s_{23} & c_{23} \end{pmatrix} \begin{pmatrix} c_{13} & 0 & s_{13} e^{-i\delta_{CP}} \\ 0 & 1 & 0 \\ -s_{13} e^{i\delta_{CP}} & 0 & c_{13} \end{pmatrix} \begin{pmatrix} c_{12} & s_{12} & 0 \\ -s_{12} & c_{12} & 0 \\ 0 & 0 & 1 \end{pmatrix}$$

where, $c_{ij} = \cos \theta_{ij}$ and $s_{ij} = \sin \theta_{ij}$.

$$P(\nu_\alpha \rightarrow \nu_\beta) = \left| U_{\beta 1} U_{\alpha 1}^* + U_{\beta 2} U_{\alpha 2}^* e^{-i 2 \alpha \Delta} + U_{\beta 3} U_{\alpha 3}^* e^{-i 2 \Delta} \right|^2$$

$$\text{where, } \Delta m_{ij}^2 = m_i^2 - m_j^2, \quad \alpha = \frac{\Delta m_{21}^2}{\Delta m_{31}^2} \quad \text{and} \quad \Delta = \frac{\Delta m_{31}^2 L}{4E}$$

In this analysis, we use three-flavor oscillation framework in the presence of matter (PREM profile) with the following values of the benchmark oscillation parameters.

| $\sin^2 2\theta_{12}$ | $\sin^2 \theta_{23}$ | $\sin^2 2\theta_{13}$ | $ \Delta m_{32}^2 (\text{eV}^2)$ | $\Delta m_{21}^2 (\text{eV}^2)$ | δ_{CP} | Mass Ordering |
|-----------------------|----------------------|-----------------------|-----------------------------------|---------------------------------|---------------|---------------|
| 0.855 | 0.5 | 0.0875 | 2.46×10^{-3} | 7.4×10^{-5} | 0 | Normal (NO) |

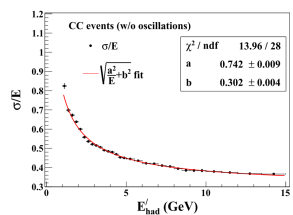
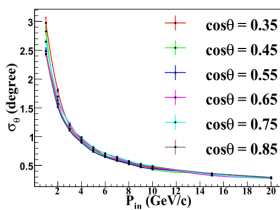
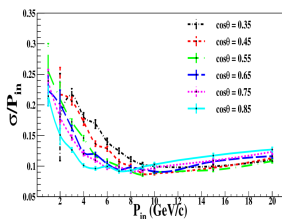
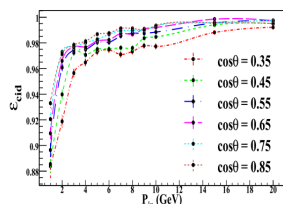
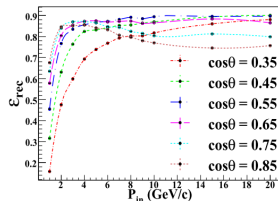
- Normal Ordering (NO): $(m_3^2 > m_2^2 > m_1^2)$
- Inverted Ordering (IO): $(m_2^2 > m_1^2 > m_3^2)$

$$\Delta m_{\text{eff}}^2 = \Delta m_{31}^2 - \Delta m_{21}^2 (\cos^2 \theta_{12} - \cos \delta_{CP} \sin \theta_{13} \sin 2\theta_{12} \tan \theta_{23})$$

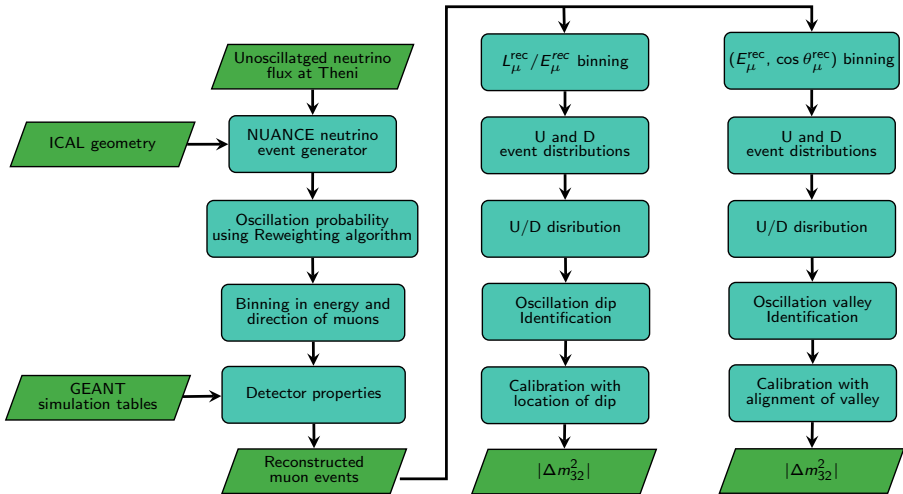
Backup: Detector Response of ICAL

In CC events at ICAL:

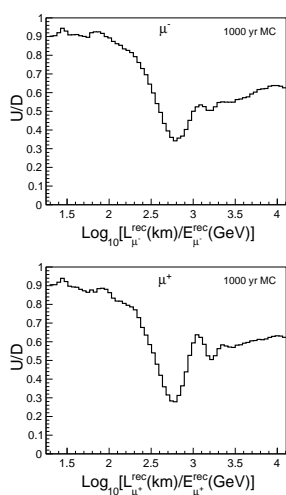
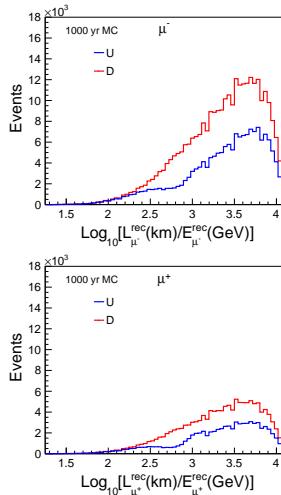
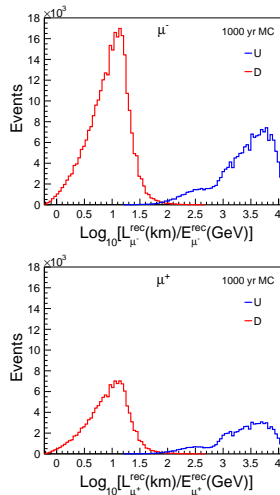
- Muon \rightarrow track-like events
- Hadron \rightarrow shower-like events



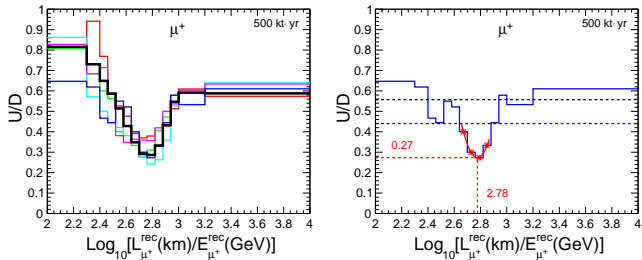
Backup: Event Generation at ICAL Detector



Backup: Events and U/D Ratio Using 1000-year MC Simulation



Backup: Identifying the dip



- The left panel shows 5 representative set of 10-year simulated data and thick black line shows mean of 100 simulated sets of 10-year data.
- The right panel shows dip identification algorithm where we start with initial ratio threshold which is shown as dashed black line.
- If ratio threshold passes through more than one dip then we decrease the ratio threshold.
- The blue dashed line shows the final ratio threshold which passes through only single oscillation dip.
- The bins with U/D ratio less than final ratio threshold are fitted with parabola to obtain location of dip.

Backup: Variation of oscillation parameters

We first simulated 100 statistically independent unoscillated data sets. Then for each of these data sets, we take 20 random choices of oscillation parameters, according to the gaussian distributions

$$\Delta m_{21}^2 = (7.4 \pm 0.2) \times 10^{-5} \text{ eV}^2, \Delta m_{32}^2 = (2.46 \pm 0.03) \times 10^{-5} \text{ eV}^2, \\ \sin^2 2\theta_{12} = 0.855 \pm 0.020, \sin^2 2\theta_{13} = 0.0875 \pm 0.0026, \sin^2 \theta_{23} = 0.50 \pm 0.03,$$

guided by the present global fit. We keep $\delta_{CP} = 0$, since its effect on ν_μ survival probability is known to be highly suppressed in the multi-GeV energy range. This procedure effectively enables us to consider the variation of our results over 2000 different combinations of oscillation parameters, to take into account the effect of their uncertainties.

Backup: Systematics uncertainties

The five uncertainties are (i) 20% in overall flux normalization, (ii) 10% in cross sections, (iii) 5% in the energy dependence, (iv) 5% in the zenith angle dependence, and (v) 5% in overall systematics.

For each of the 2000 simulated data sets, we modify the number of events in each $(E_\mu^{\text{rec}}, \cos \theta_\mu^{\text{rec}})$ bin as

$$N = N^{(0)}(1 + \delta_1)(1 + \delta_2)(E_\mu^{\text{rec}}/E_0)^{\delta_3}(1 + \delta_4 \cos \theta_\mu^{\text{rec}})(1 + \delta_5) ,$$

where $N^{(0)}$ is the theoretically predicted number of events, and $E_0 = 2$ GeV. Here $(\delta_1, \delta_2, \delta_3, \delta_4, \delta_5)$ is an ordered set of random numbers, generated separately for each simulated data set, with the gaussian distributions centred around zero and the 1σ widths given by $(20\%, 10\%, 5\%, 5\%, 5\%)$.

Backup: Existing bounds on $\varepsilon_{\mu\tau}$

| Experiment | 90% C.L. bounds | |
|------------------------|--|---|
| | Their Convention ($\tilde{\varepsilon}_{\mu\tau}$) | Our convention ¹⁴ ($\varepsilon_{\mu\tau} = 3\tilde{\varepsilon}_{\mu\tau}$) |
| IceCube ¹⁵ | $-0.006 < \tilde{\varepsilon}_{\mu\tau} < 0.0054$ | $-0.018 < \varepsilon_{\mu\tau} < 0.0162$ |
| DeepCore ¹⁶ | $-0.0067 < \tilde{\varepsilon}_{\mu\tau} < 0.0081$ | $-0.0201 < \varepsilon_{\mu\tau} < 0.0243$ |
| Super-K ¹⁷ | $ \tilde{\varepsilon}_{\mu\tau} < 0.011$ | $ \varepsilon_{\mu\tau} < 0.033$ |

Table: Existing bounds on $\varepsilon_{\mu\tau}$ at 90% confidence level. Note that the bounds presented are on $\tilde{\varepsilon}_{\mu\tau}$ that is defined according to the convention

$V_{\text{NSI}} = \sqrt{2}G_F N_d \tilde{\varepsilon}_{\mu\tau}$, while we use the convention $V_{\text{NSI}} = \sqrt{2}G_F N_e \varepsilon_{\mu\tau}$. Since $N_d \approx 3N_e$ in Earth, the bounds on $\tilde{\varepsilon}_{\mu\tau}$ have been converted to the bounds on $\varepsilon_{\mu\tau}$, using $\varepsilon_{\mu\tau} = 3\tilde{\varepsilon}_{\mu\tau}$, as shown in the third column.

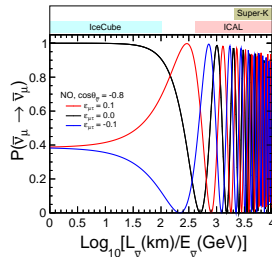
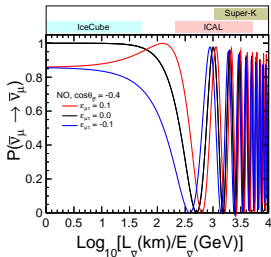
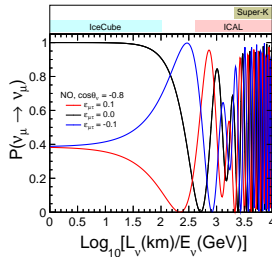
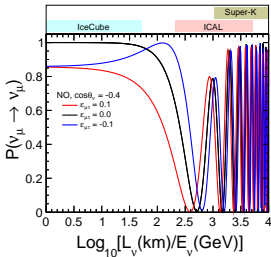
¹⁴Y. Farzan and M. Tortola, Front. in Phys. 6 (2018) 10, arXiv:1710.09360.

¹⁵J. Salvado, et. al., JHEP 01 (2017) 141, arXiv:1609.03450

¹⁶IceCube collaboration, Phys. Rev. D 97 (2018) 072009, arXiv:1709.07079

¹⁷Super-Kamiokande collaboration, Phys. Rev. D 84 (2011) 113008, arXiv:1109.1889

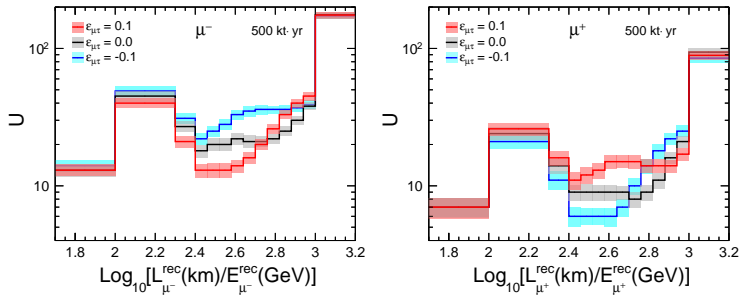
Backup: $P(\nu_\mu \rightarrow \nu_\mu)$ in presence of NSI



Location of dip shifts in the presence of NSI.

Anil Kumar et al., JHEP 04 (2021) 159., arXiv: 2101.02607

Backup: Event distribution in presence of NSI



Anil Kumar et al., JHEP 04 (2021) 159., arXiv: 2101.02607